Electronic Supplementary Information

Rational Design of Phenoxazine-based Donor-Acceptor-Donor Thermally Activated Delayed Fluorescence Molecules with High Performance

Jing Lu, Yiying Zheng, and Jingping Zhang*

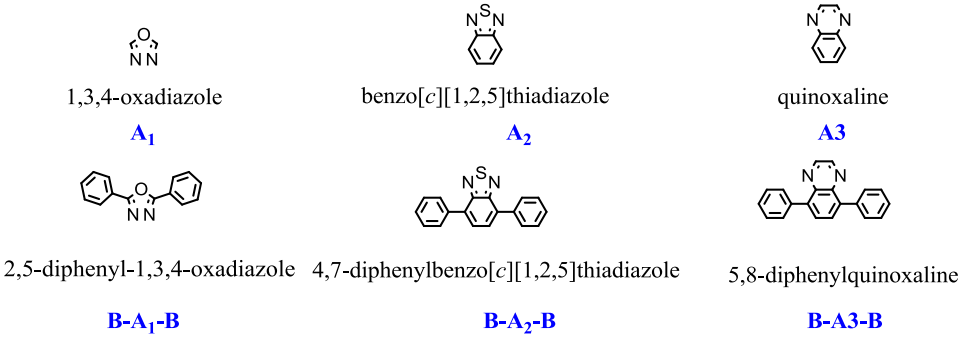

Fig. S1 The chemical structures of these investigated acceptors.

Methodology

Table S1 The calculated ΔE_{ST} values of D-B-A_1-B-D in toluene using TD-DFT method.

	B3LYP	CAM-B3LYP	PBE0	Expt.[1]
ΔE_{ST}	0.01	0.54 [0.57][1]	**0.13**	**0.15**

[1] The data come from Ref. [22]

Firstly, we optimized the first singlet (S_1) and triplet (T_1) excited states using TD-B3LYP, TD-CAM-B3LYP, and TD-PBE0 with cc-pVDZ basis set, respectively. Secondly, on the basis of the optimized S_1 and T_1 states, the relative singlet and triplet excitation energy levels were computed using polarizable continuum model (PCM) in toluene. The calculated ΔE_{ST} values are listed in Table S1, the most suitable method is found to be PBE0, which provides the closest ΔE_{ST} to experimental value.

The choice of acceptors

Table S2 The calculated energy levels of HOMO (H) and LUMO (L) for donor (D) and different acceptors (As).

	D	B-A_1-B	A_1	B-A_2-B	A_2	B-A_3-B	A_3

E (L)	-0.317	**-1.645**	-0.346	**-2.574**	-2.307	**-2.037**	-1.932
E (H)	-5.051	**-6.507**	-8.145	**-6.003**	-6.977	**-6.219**	-7.089
ΔE_L		**1.328**	0.028	**2.257**	1.989	**1.719**	1.615
ΔE_H		**1.456**	3.094	**0.951**	1.938	**1.168**	2.038

The optimized structural parameters

Table S3a The optimized bond length (Å), bond angle (°), and dihedral angle (°) of the A_i, B-A_i-B, D-B-A_i-B, and D-B-A_i-B-D (i=1-3).

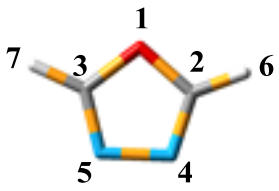 **A_1**		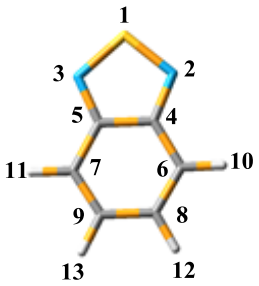 **A_2**		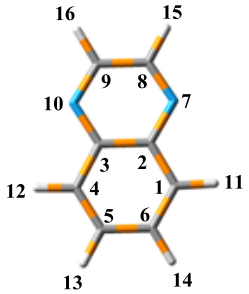 **A_3**	
R(1, 2)	1.350	**R(1, 2)**	1.639	**R(1, 2)**	1.416
R(1, 3)	1.350	**R(1, 3)**	1.639	**R(2, 3)**	1.426
R(2, 4)	1.289	**R(2, 4)**	1.336	**R(3, 4)**	1.416
R(3, 5)	1.289	**R(3, 5)**	1.336	**R(4, 5)**	1.375
R(4, 5)	1.386	**R(4, 5)**	1.446	**R(5, 6)**	**1.417**
R(2, 6)	1.086	**R(4, 6)**	1.423	**R(6, 1)**	**1.375**
R(3, 7)	1.086	**R(5, 7)**	1.423	**R(2, 7)**	1.361
α (1, 2, 6)	118.1	**R(6, 8)**	1.369	**R(7, 8)**	1.312
α (1, 3, 7)	118.1	**R(7, 9)**	1.369	**R(8, 9)**	1.419
		R(8, 9)	1.430	**R(9, 10)**	1.312
		α (4, 6, 10)	119.6	**R(10, 3)**	1.361
		α (5, 7, 11)	119.6	**α (2, 1, 11)**	117.7
				α (3, 4, 12)	**117.7**
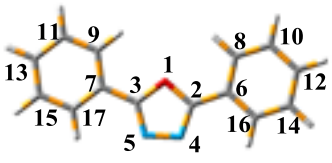 **B-A_1-B**		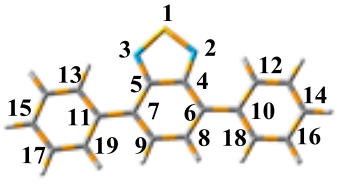 **B-A_2-B**		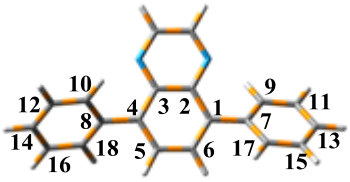 **B-A_3-B**	

R(1, 2)	1.356	**R(1, 2)**	1.632	**R(1, 2)**	1.431
R(1, 3)	1.356	**R(1, 3)**	1.632	**R(2, 3)**	1.433
R(2, 4)	1.300	**R(2, 4)**	1.335	**R(3, 4)**	1.431
R(3, 5)	1.300	**R(3, 5)**	1.335	**R(4, 5)**	1.383
R(4, 5)	1.369	**R(4, 5)**	1.463	**R(5, 6)**	1.407
R(2, 6)	1.454	**R(4, 6)**	1.442	**R(6, 1)**	1.383
R(3, 7)	1.454	**R(5, 7)**	1.442	**R(1, 7)**	1.481
α (1, 2, 6)	119.9	**R(6, 8)**	1.381	**R(7, 9)**	1.403
α (1, 3, 7)	119.9	**R(7, 9)**	1.381	**R(9, 11)**	1.391
β (1,2,6,8)	0.0	**R(8, 9)**	1.413	**R(11, 13)**	1.394
β (1,3,7,9)	0.0	**α (4, 6, 10)**	124.8	**R(13, 15)**	1.393
		α (5, 7, 11)	124.8	**R(15, 17)**	1.393
		β (4,6,10,12)	0.0	**R(17, 7)**	1.403
		β (5,7,11,13)	0.0	**α (2, 1, 7)**	122.7
				β (2,1,7,9)	-46.8

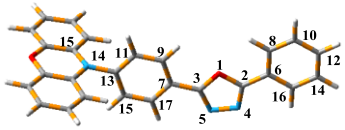

D-B-A_1-B

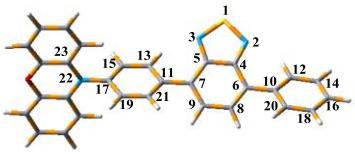

D-B-A_2-B

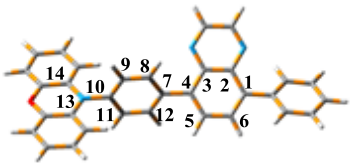

D-B-A_3-B

R(1, 2)	1.357	**R(1, 2)**	1.635	**R(1, 2)**	1.432
R(1, 3)	1.356	**R(1, 3)**	1.636	**R(2, 3)**	1.432
R(2, 4)	1.301	**R(2, 4)**	1.335	**R(3, 4)**	1.431
R(3, 5)	1.300	**R(3, 5)**	1.335	**R(4, 5)**	1.383
R(4, 5)	1.369	**R(4, 5)**	1.452	**R(5, 6)**	1.407
R(2, 6)	1.454	**R(4, 6)**	1.436	**R(6, 1)**	1.383
R(3, 7)	1.454	**R(5, 7)**	1.436	**R(4, 7)**	1.481
α (1, 2, 6)	119.9	**R(6, 8)**	1.378	**R(7, 8)**	1.403
α (1, 3, 7)	119.9	**R(7, 9)**	1.379	**R(8, 9)**	1.390
β (1,2,6,8)	-0.1	**R(8, 9)**	1.419	**R(9, 10)**	1.396
β (1,3,7,9)	-0.2	**α (4, 6, 10)**	122.9	**R(10, 11)**	1.395
β (11,13,14,15)	93.0	**α (5, 7, 11)**	122.9	**R(11, 12)**	1.392
		β (4,6,10,12)	-37.5	**R(12, 7)**	1.403
		β (5,7,11,13)	36.4	**α (3, 4, 7)**	122.5

		β (15,17,22,23)	-90.1	**β (3,4,7,8)**	-46.5
				α (9, 10, 13)	120.3
				β (9,10,11,13)	88.9
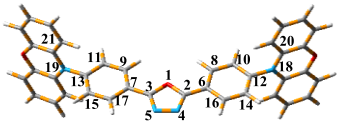		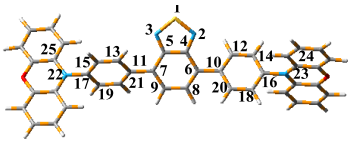		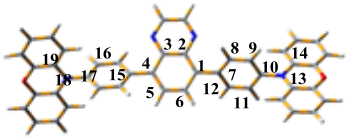	
D-B-A_1-B-D		**D-B-A_2-B-D**		**D-B-A_3-B-D**	
R(1, 2)	1.356	**R(1, 2)**	1.635	**R(1, 2)**	1.383
R(1, 3)	1.356	**R(1, 3)**	1.635	**R(2, 3)**	1.407
R(2, 4)	1.300	**R(2, 4)**	1.335	**R(3, 4)**	1.383
R(3, 5)	1.300	**R(3, 5)**	1.335	**R(4, 5)**	1.431
R(4, 5)	1.368	**R(4, 5)**	1.451	**R(5, 6)**	1.431
R(2, 6)	1.454	**R(4, 6)**	1.436	**R(6, 1)**	1.431
R(3, 7)	1.454	**R(5, 7)**	1.436	**R(1, 7)**	1.481
R(12, 18)	1.422	**R(6, 8)**	1.379	**R(7, 8)**	1.403
R(13, 19)	1.422	**R(7, 9)**	1.379	**R(8, 9)**	1.390
α (1, 2, 6)	119.9	**R(8, 9)**	1.420	**R(9, 10)**	1.396
α (1, 3, 7)	119.9	**R(17, 22)**	1.423	**R(10, 11)**	1.395
β (1,2,6,8)	-0.1	**R(16, 23)**	1.423	**R(11, 12)**	1.392
β (1,3,7,9)	-0.1	**α (4, 6, 10)**	122.7	**R(12, 7)**	1.403
β (11,13,19,21)	-87.4	**α (5, 7, 11)**	122.7	**α (2, 1, 7)**	122.4
β (10,12,18,20)	87.4	**β (4,6,10,12)**	-38.4	**α (3, 4, 15)**	122.4
		β (5,7,11,13)	-38.4	**β (16,17,18,19)**	89.1
		β (14,16,23,24)	85.3	**β (9, 10, 13,14)**	-89.1
		β (15,17,22,25)	85.3		

Table S3b The optimized bond length (Å), bond angle (°), and dihedral angle (°) of the D-A_i-D (i=2, 3).

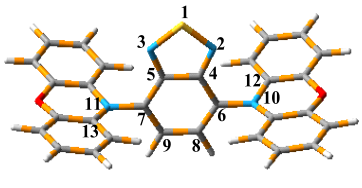		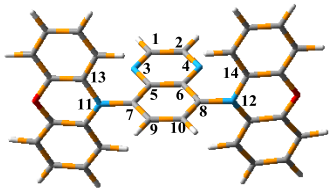	
D-A_2-D		**D-A_3-D**	
R(1, 2)	1.636	**R(1, 2)**	1.420
R(1, 3)	1.636	**R(1, 3)**	1.312

R(2, 4)	1.334	**R(2, 4)**	1.312
R(3, 5)	1.334	**R(3, 5)**	1.357
R(4, 6)	1.443	**R(4, 6)**	1.357
R(5, 6)	1.432	**R(5, 6)**	1.424
R(5, 7)	1.432	**R(5, 7)**	1.428
R(6, 8)	1.371	**R(6, 8)**	1.428
R(7, 9)	1.371	**R(7, 9)**	1.376
R(8, 9)	1.427	**R(8, 10)**	1.376
R(6, 10)	1.415	**R(9, 10)**	1.414
R(7, 11)	1.415	**R(7, 11)**	1.418
α (4, 6, 10)	120.9	**R(8, 12)**	1.418
α (5, 7, 11)	120.9	**α (5, 7, 11)**	120.0
β (4,6,10,12)	-79.4	**α (6, 8, 12)**	120.0
β(5,7,11,13)	-79.4	**β(5,7,11,13)**	-81.1
		β (6,8,12,14)	81.1

Singlet-triplet energy gap

In Table S2, The LUMO energy level of A_1 is similar with that of D, indicating that the match between A_1 and D is not expected. However, A_2, and A_3 moieties can be also as strong electron withdrawing fragments with lower LUMO energy levels, even if the electron withdrawing strength are weaker than relative B-A_i-B due to shortening the π-conjugation. As a comparison, we calculated the ΔE_{ST} values for the D-A_i-D (i=2, 3) topologic molecules. The calculated twist angles between D and A are within 79.4° and -81.1° for D-A_i-D (i=2, 3) from the optimized geometries in S_0 states by DFT, respectively. The electron density plots of HOMO and LUMO are also exhibited an effective separation between A_i and D fragments. Thus the D-A_i-D molecules are also as efficient TADF candidates. The calculated ΔE_{ST} values for D-A_i-D are 0.13 eV and 0.26 eV, respectively, which are larger than relative D-B-A_i-B-D ones due to the reducing of electron withdrawing strength.

Frontier molecular orbital

Table S4 The electron density plots of fronrier molecular orbitals and the percentage of electronic distribution.

		D	**B**	**A_i**	**B**	**D**	
D-B-A_1-B	**L**	1.4	40.5	34.3	23.8		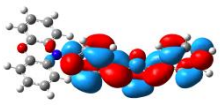

	H	97.4	2.6	0.0	0.0		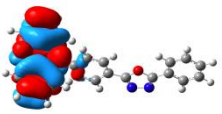
D-B-A$_1$-B-D	**L**	1.1	32.0	33.9	32.0	1.1	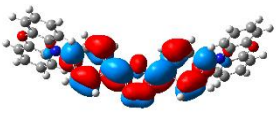
	H	0.0	0.0	0.0	2.6	97.4	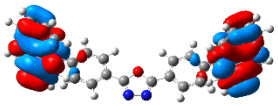
D-B-A$_2$-B	**L**	0.0	6.3	88.4	5.3		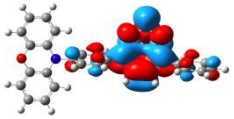
	H	97.4	2.6	0.0	0.0		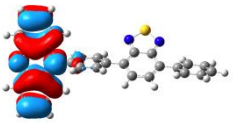
D-B-A$_2$-B-D	**L**	0.2	5.8	88.1	5.8	0.2	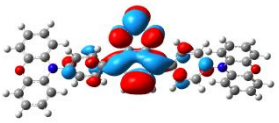
	H	48.6	1.4	0.0	1.4	48.6	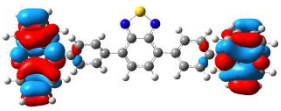
D-B-A$_3$-B	**L**	0.2	5.5	89.9	4.4		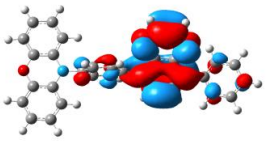
	H	97.4	2.6	0.0	0.0		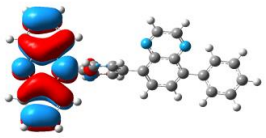
D-B-A$_3$-B-D	**L**	0.2	5.3	89.0	5.3	0.2	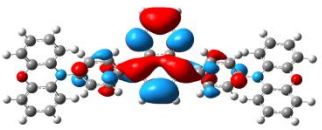
	H	50.9	1.3	0.0	1.3	46.5	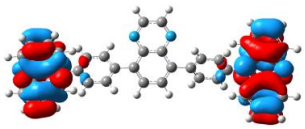
D-A$_2$-D	**L**	0.9	-	98.3	-	0.9	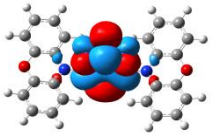

	H	48.6	-	2.8	-	48.6	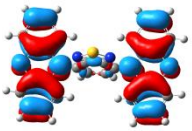
D-A$_3$-D	**L**	0.9	-	98.1	-	0.9	
	H	48.5	-	3.0	-	48.5	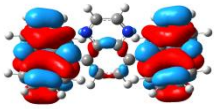

Table S5 The overlap of electronic transition density.

					
		D_1 & B_1	B_1 & A_i	A_i & B_2	B_2 & D_2
D-B-A$_1$-B-D	L	**0.017**	**0.042**	**0.042**	**0.017**
	H	0.000	0.000	0.000	**0.007**
D-B-A$_2$-B-D	L	**0.006**	**0.003**	**0.008**	**0.003**
	H	**0.014**	0.000	0.000	**0.004**
D-B-A$_3$-B-D	L	**0.003**	**0.010**	**0.010**	**0.003**
	H	**0.004**	0.000	0.000	**0.004**

The percentages of electronic distribution of LUMOs and HOMOs on different fragments for all these investigated compounds were computed by the PyMOlyze 1.1 program.

Table S6 The calculated the atomic charges of the investigated D-B-A$_i$-B-D molecules in the ground (S_0) and singlet excited (S_1) states using NPA method.

			
		B_1-A_i-B_2	D_1 (D_2)
D-B-A$_1$-B-D	S_0	0.452	-0.226 (-0.226)
	S_1	0.457	-0.228 (-0.229)
	$\Delta^{[1]}$	**-0.005**	**0.002 (0.003)**
D--B-A$_2$-B-D	S_0	0.468	-0.234 (-0.234)
	S_1	0.478	-0.241 (-0.237)
	Δ	**-0.010**	**0.007 (0.003)**
D-B-A$_3$-B-D	S_0	0.472	-0.236 (-0.236)

S_1	0.481	-0.241 (-0.240)
Δ	**-0.009**	**0.005 (0.004)**

[1]The charge differences between S_0 and S_1 states.

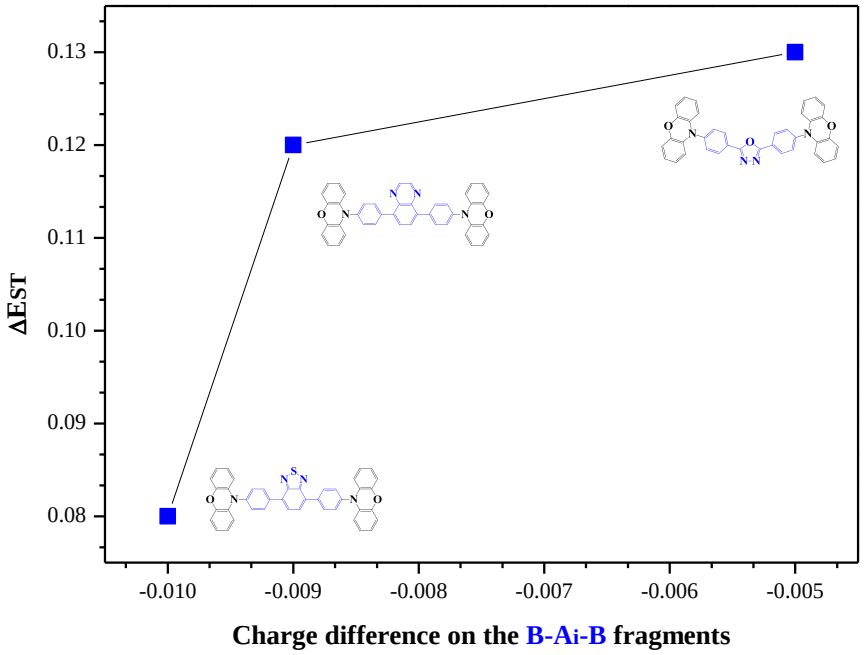

Fig. S2 The ΔE_{ST} values as a function of the charge difference on the B-A_i-B fragments.

Reorganization energy

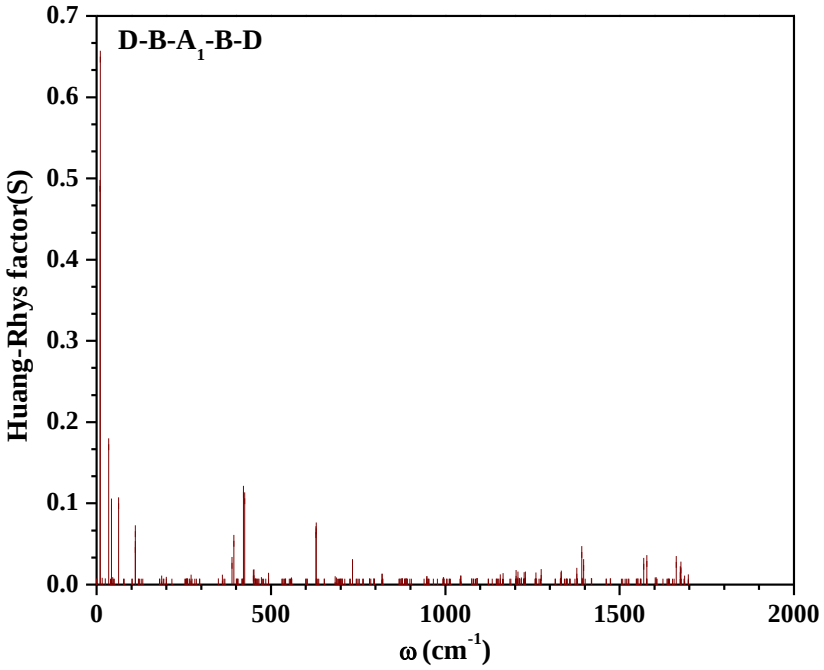
D-B-A1-B-D
Huang-Rhys factor(S)
0.0
0.1
0.2
0.3
0.4
0.5
0.6
0.7
0
500
1000
1500
2000
ω (cm-1)

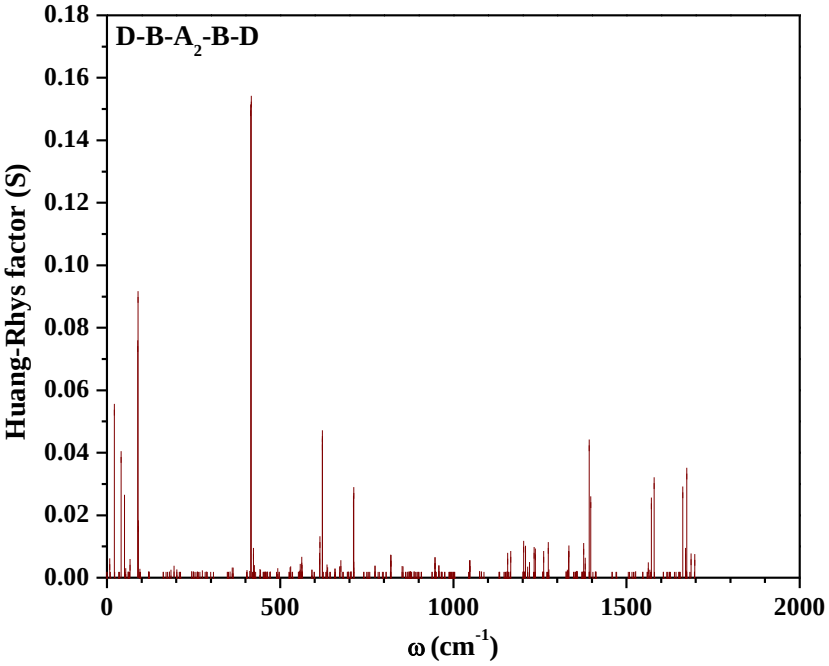
D-B-A2-B-D
Huang-Rhys factor (S)
0.00
0.02
0.04
0.06
0.08
0.10
0.12
0.14
0.16
0.18
0
500
1000
1500
2000
ω (cm-1)

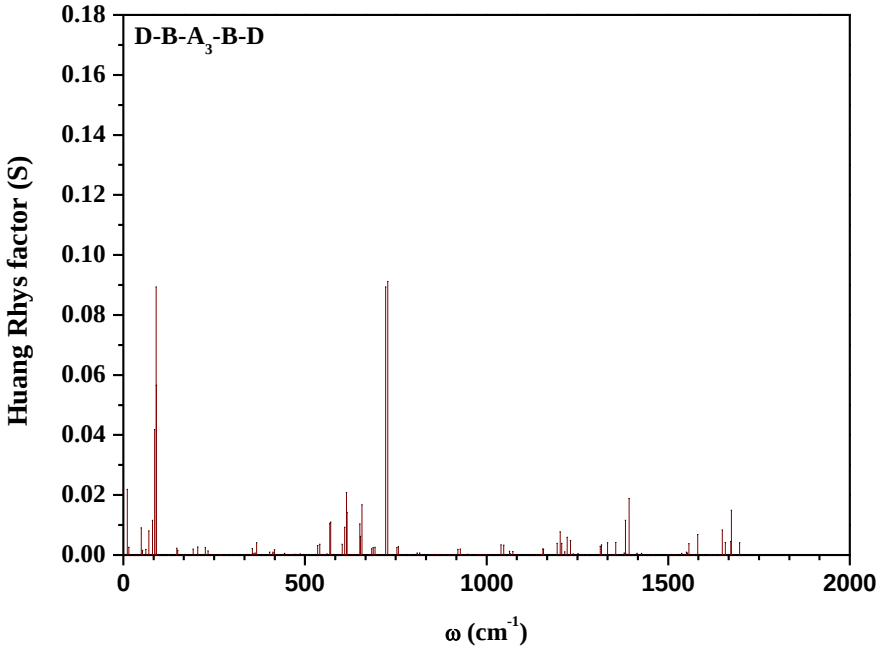

Fig. S3 The theoretical estimated Huang-Rhys factor (*S*) for all studied D-B-A_i-B-D molecules.

Table S7a The calculated hole reorganization energy via potential energy surface (PES) and normal mode (NM) analysis.

λ_h	D-B-A_1-B-D	D-B-A_2-B-D	D-B-A_4-B-D
PES	0.100	0.094	0.075
NM	0.097	0.094	0.075

Table S7b The DFT estimates of vertical and adiabatic ionization potentials (IP_v and IP_a), electronic affinities (EA_v and EA_a), hole and electron extraction potential (HEP and EEP), reorganization energies (λ_h and λ_e) (energies in eV).

	IP_V	IP_a	EA_v	EA_a	HEP	EEP	λ_h	λ_e
	6.218 [a]	6.096	0.467	0.645	6.014	0.778	0.204	0.311
D-B-A_1-B	6.437 [b]	6.330	0.677	0.836	6.229	0.996	0.207	0.320
	6.507 [c]	6.395	0.443	0.615	6.285	0.825	0.222	0.382
	6.066	5.945	1.073	1.277	5.869	1.485	0.197	0.412
D-B-A_2-B	6.286	6.187	1.281	1.507	6.086	1.714	0.200	0.434
	6.351	6.245	1.173	1.392	6.138	1.629	0.213	0.457
	6.035	5.922	0.693	1.081	5.858	1.254	0.177	0.561
D-B-A_3-B	6.257	6.160	0.933	1.164	60.61	1.393	0.196	0.460
	6.321	6.219	0.777	0.997	6.112	1.255	0.210	0.477

Table S8 The selected hole reorganization energies $\lambda_h(j)$, Huang-Rhys factor (S), associated with vibrational mode (ω) using NM analysis (in cm-1).

	D-B-A_1-B-D		**D-B-A_2-B-D**		**D-B-A_3-B-D**	
ω	$\lambda_{h(j)}$	***S***	$\lambda_{h(j)}$	***S***	$\lambda_{h(j)}$	***S***
388-394	31.7	0.081	-	-	-	-
415-427	93.2	0.220	129.6	0.312	0.8	0.002
614-657	84.2	0.134	68.4	0.111	21.6	0.035
712-735	34.0	0.046	39.0	0.055	131.0	0.181
1203-1230	46.3	0.038	37.7	0.031	28.8	0.024
1274-1333	38.5	0.029	14.7	0.012	14.1	0.014
1376-1397	110.8	0.080	112.2	0.121	43.7	0.044
1568-1581	86.6	0.055	85.3	0.054	10.9	0.007
1662-1676	131.7	0.079	115.1	0.070	32.7	0.020

Mobility

Table S9 The hole and electron mobility of D-B-A_1-B-D via FGR and Marcus theory at the different temperature.

T	μ_{hole} **(cm^2/Vs)**	$\mu_{electron}$ **(cm^2/Vs)**	μ_{hole} **(cm^2/Vs)**	$\mu_{electron}$ **(cm^2/Vs)**
	FGR		**Marcus**	
300 K	0.00281	0.01075	0.001465	0.0028166
298.15 K	**0.00285**	**0.01085**	**0.0014698**	**0.0027905**
250 K	0.00395	0.01419	0.0015871	0.0020328
200 K	0.00594	0.02016	0.0016595	0.0011558
150 K	0.00989	0.0327	0.0015754	0.00039745
100 K	0.01978	0.06815	0.0011003	0.000036427
50 K	0.05975	0.23499	0.00017103	0.000000012794

Table S10 The main hole and electron transfer integrals (V_h and V_e) for the main three nearest pathways of D-B-A_i-B-D.

	Distance (Å)	V_h	V_e
D-B-A_1-B-D	9.068	0.000074504	-0.0032
	7.599	-0.0014	0.0077
	7.984	0.000017480	0.0065

D-B-A_2-B-D	3.876	0.0121	0.2041
	3.876	0.0121	0.2041
	12.690	-0.0023	-0.000030478
D-B-A_3-B-D	4.410	-0.0141	0.0267
	7.193	-0.0617	-0.0897
	5.331	-0.0169	-0.0168

Normal mode analysis

D-B-A_1-B-D (2PXZ-OXD)			**D-B-A_2-B-D**		
ω (cm^{-1})	**$\lambda_{h(i)}$ (cm^{-1})**	***S***	**ω (cm^{-1})**	**$\lambda_{h(i)}$ (cm^{-1})**	***S***
10	4.9	0.49104	21	1.1	0.05379
11	7.4	0.6498	41	1.6	0.03864
35	6	0.17287	51	1.3	0.02464
43	4.2	0.09857	54	0.1	0.00115
46	0.1	0.00192	67	0.3	0.00414
63	6.4	0.10035	89	6.6	0.07411
111	5.1	0.04621	90	8.1	0.08989
111	7.3	0.06588	91	1.5	0.01656
187	0.7	0.00378	95	0.1	9.68E-04
200	0.5	0.00238	185	0.1	6.48E-04
258	0.1	4.50E-04	194	0.4	0.00198
260	0.1	3.13E-04	202	0.2	8.00E-04
271	1.3	0.0049	275	0.1	4.81E-04
349	0.1	2.42E-04	362	0.5	0.00135
361	1.8	0.0051	364	0.5	0.00135
388	10.5	0.02691	404	0.2	5.45E-04
394	21.2	0.05379	412	0.1	2.88E-04
421	48.1	0.11424	415	62	0.1496
425	45.1	0.10626	417	63.5	0.15235
450	5	0.01125	423	3.2	0.00769
451	5.2	0.01155	426	0.9	0.00218
473	0.8	0.00174	442	0.4	8.82E-04
493	3.5	0.00708	443	0.3	7.22E-04
555	0.1	9.80E-05	493	0.6	0.0012
559	0.8	0.00146	529	0.8	0.00151
629	40.7	0.0648	530	0.9	0.00174
630	43.5	0.06919	555	0.2	2.88E-04

684	2	0.00289	558	1.5	0.00259
688	1	0.00151	562	2.7	0.0048
712	0.1	1.28E-04	563	1.2	0.00224
712	0.1	1.45E-04	592	0.4	7.22E-04
734	16.2	0.02205	592	0.4	6.85E-04
735	17.6	0.02398	614	3.7	0.00605
783	0.2	3.13E-04	615	7	0.0114
795	0.3	3.92E-04	622	26.5	0.04263
818	4.8	0.00594	622	28.2	0.0453
819	5	0.00605	635	1.5	0.00238
876	0.2	2.00E-04	637	0.9	0.00146
876	0.6	7.22E-04	658	0.6	9.68E-04
888	0.8	9.25E-04	658	0.7	0.00106
947	2.9	0.00304	672	1.1	0.00174
947	3	0.00312	675	2.5	0.0037
994	1.6	0.00168	697	0.1	1.13E-04
995	1.7	0.00174	705	0.2	2.42E-04
1044	4.1	0.00387	712	17.4	0.02442
1045	4.2	0.00396	713	2.3	0.0032
1076	0.4	3.65E-04	713	19.3	0.02714
1081	0.1	6.05E-05	774	1.5	0.00198
1090	0.6	5.78E-04	774	1.5	0.00198
1092	0.6	5.78E-04	819	4.5	0.00551
1158	0.6	5.45E-04	820	4.4	0.00541
1158	6.4	0.00551	852	1.6	0.00186
1166	7.9	0.00684	855	1.5	0.00174
1185	0.1	5.00E-05	875	0.1	8.45E-05
1203	12.8	0.01066	876	0.2	1.81E-04
1208	10.6	0.00871	887	0.2	1.81E-04
1213	0.7	5.78E-04	947	4.3	0.00461
1218	1.8	0.00146	947	4.5	0.0047
1226	9.7	0.00794	948	0.2	2.65E-04
1230	10.7	0.00871	958	2	0.00211
1260	0.3	2.42E-04	959	2	0.00211
1260	9.5	0.00756	1047	3.9	0.0037
1275	14.8	0.0117	1048	3.9	0.0037
1332	10.6	0.00794	1076	0.3	3.13E-04
1333	13.1	0.0098	1081	0.1	6.05E-05
1342	0.1	5.00E-05	1154	0.1	5.00E-05

1377	18.6	0.01345
1378	0.4	2.65E-04
1391	56.1	0.04033
1392	1.8	0.0013
1397	33.9	0.0242
1419	1.1	7.61E-04
1420	0.5	3.13E-04
1473	0.6	3.92E-04
1474	0.5	3.65E-04
1526	0.2	1.62E-04
1549	0.2	1.45E-04
1552	0.6	3.65E-04
1569	40.5	0.02576
1578	0.1	3.20E-05
1578	46	0.02904
1602	2.1	0.00135
1605	3.2	0.00198
1662	46.4	0.02785
1674	25.3	0.01514
1675	19.6	0.0117
1676	35.1	0.02101
1686	6.6	0.00396
1697	8.9	0.0052
3173	0.6	2.00E-04
3184	0.6	1.81E-04

1157	7	0.00605
1166	7.9	0.00673
1201	0.1	1.28E-04
1203	12	0.00994
1205	0.1	5.00E-05
1208	10	0.00832
1215	2	0.00168
1220	3.8	0.00312
1233	9.8	0.00794
1237	9.3	0.00744
1258	0.1	8.45E-05
1261	8.5	0.00673
1274	12.1	0.00952
1276	1	7.61E-04
1326	0.3	2.42E-04
1329	0.9	6.85E-04
1330	0.4	3.38E-04
1332	0.2	1.62E-04
1333	9	0.00673
1334	11.3	0.00845
1356	0.4	2.65E-04
1358	0.5	3.38E-04
1372	0.2	1.28E-04
1376	0.4	2.65E-04
1376	12.7	0.00925
1379	0.2	1.45E-04
1381	6.2	0.00451
1392	58.8	0.04234
1397	33.9	0.0242
1410	0.1	6.05E-05
1412	0.1	5.00E-05
1526	0.3	1.81E-04
1563	4.7	0.00304
1567	1	6.48E-04
1572	37.4	0.02376
1580	47.9	0.03026
1662	45.7	0.02738
1670	12.8	0.00769
1672	0.8	4.81E-04

1674	55.8	0.03328
1686	10	0.00594
1697	9.8	0.00572
3173	0.2	5.00E-05
3174	0.5	1.62E-04
3184	0.1	3.20E-05
3185	0.5	1.62E-04

D-B-A_3-B-D

ω (cm^{-1})	**$\lambda_{h(i)}$ (cm^{-1})**	***S***
15	0.05	0.0026
11	0.25	0.0219
49	0.45	0.00912
53	0.1	0.0016
62	0.1	0.00194
70	0.55	0.0081
80	0.95	0.01166
86	3.6	0.04182
90	8.05	0.0894
91	5.15	0.05664
147	0.35	0.0023
150	0.25	0.0016
192	0.4	0.00207
205	0.55	0.00276
226	0.6	0.00255
233	0.35	0.00144
246	0.05	1.00E-04
268	0.05	1.00E-04
290	0.05	2.40E-04
355	0.8	0.00226
357	0.2	6.25E-04
363	0.25	7.29E-04
367	1.5	0.00416
403	0.4	0.00102
411	0.2	4.41E-04
412	0.45	0.00106
416	0.75	0.00185
422	0.05	1.69E-04
427	0.05	1.10E-04
443	0.15	3.42E-04

444	0.25	5.76E-04
456	0.05	7.23E-05
458	0.05	1.21E-04
472	0.15	2.72E-04
484	0.05	1.44E-04
487	0.2	3.61E-04
494	0.1	2.10E-04
535	1.7	0.00319
541	2	0.00366
561	0.2	3.80E-04
568	6	0.01061
571	6.3	0.01102
603	2.15	0.0036
609	5.7	0.00931
614	12.8	0.02088
616	8.8	0.01428
629	0.05	4.90E-05
651	6.75	0.0104
653	0.75	0.00116
653	4.1	0.00624
657	11.05	0.01677
684	1.45	0.00216
688	1.7	0.0025
693	1.8	0.0026
713	0.1	1.10E-04
722	64.45	0.0894
728	66.45	0.0912
753	1.9	0.0025
757	2.2	0.00286
809	0.6	7.56E-04
816	0.6	7.29E-04
836	0.1	1.21E-04
839	0.05	5.63E-05
865	0.05	4.23E-05
921	1.75	0.00189
928	1.9	0.00202
940	0.15	1.44E-04
943	0.2	1.96E-04
948	0.3	3.24E-04

1040	3.55	0.00342
1047	3.55	0.00336
1063	1.35	0.0013
1066	0.45	4.20E-04
1072	1.3	0.00119
1081	0.15	1.21E-04
1132	0.3	2.40E-04
1139	0.25	1.96E-04
1145	0.05	3.03E-05
1155	2.45	0.00212
1157	2.15	0.00189
1193	0.05	5.63E-05
1194	4.75	0.00397
1200	0.1	9.03E-05
1203	9.45	0.00783
1207	4.8	0.00397
1215	1.35	0.00112
1222	7.3	0.00601
1231	5.9	0.00483
1239	0.45	3.61E-04
1252	0.65	5.29E-04
1253	0.05	3.03E-05
1257	0.1	6.40E-05
1260	0.1	9.03E-05
1307	0.05	2.03E-05
1313	3.8	0.00292
1316	4.5	0.00342
1325	0.1	7.23E-05
1330	0.05	2.03E-05
1333	5.55	0.00416
1339	0.05	2.03E-05
1345	0.05	3.03E-05
1347	0.05	4.90E-05
1349	0.05	2.03E-05
1356	5.75	0.00423
1360	0.05	4.23E-05
1360	0.1	7.23E-05
1370	0.15	1.10E-04
1379	1	7.29E-04

1382	16.05	0.01166
1386	0.45	3.42E-04
1392	26.25	0.01891
1414	0.8	5.76E-04
1427	0.85	6.00E-04
1455	0.1	6.40E-05
1464	0.1	7.23E-05
1516	0.2	1.21E-04
1520	0.05	2.03E-05
1537	0.85	5.76E-04
1550	1.65	0.00106
1553	1.2	7.56E-04
1557	6	0.00384
1581	10.9	0.00689
1627	0.1	6.40E-05
1640	0.1	6.40E-05
1649	13.75	0.00837
1657	6.95	0.00423
1672	0.1	4.90E-05
1672	7.6	0.00456
1674	25	0.01501
1697	6.95	0.0041